Leptonic Structure Functions measured with the L3 Detector

Klaus Dehmelt for the L3 collaboration

DESY, Notkestrasse 85, 22607 Hamburg, Germany, E-mail: klaus.dehmelt@desy.de

DOI: http://dx.doi.org/10.3204/DESY-PROC-2009-03/Dehmelt

The QED structure function F_2^γ can be rather easily extracted by means of the measurement of cross sections for electron tagged events in e^+e^- scattering. We report on a measurement of the QED structure functions of the photon with single tagged events, at Q^2 between 0.2 GeV^2 and 34 GeV^2. The data were collected with the L3 detector at LEP, for c.m.s. energies between 189 GeV and 206 GeV. The sub detectors for tagging the single beam electron were the Very Small Angle Tagger and the Luminosity detector of L3.

1 Introduction

Photons have structure and may interact with each other. This might be possible because photons can fluctuate into states of particles, which might be charged. Heisenberg's uncertainty relation $\Delta t \simeq \frac{2E_\gamma}{m^2_{pair}}$ *allows* photons to fluctuate into intermediate states, where m_{pair} represents the mass of such a state. If E_γ becomes large, Δt, i.e. the lifetime of the intermediate states can also become quite large. These intermediate states will then be responsible for the interaction of the photons and also for giving a structure to photons.
Since the fluctuation is a statistical process, the probability of the fluctuation into a particular state is described in terms of structure functions.

2 Two Photon Physics and QED

Two-photon physics nowadays is of interest, since it allows to test Quantum-Chromodynamics (QCD), the theory of strong interactions: the intermediate states might be strongly interacting particles.
Experimentally, it is very difficult to collide high energy photon beams. A very elegant way of avoiding this difficulty is the usage of virtual photons, e.g. the quantum fluctuation of an electron into an electron-photon state. Thus, high energy e^-e^+ storage rings like the Large-Electron-Positron collider (LEP) are an ideal tool for producing photons. Such accelerators can be considered as Photon-Photon colliders, since a portion of the incoming electrons (positrons) around collision points will be scattered into relatively large angles. Because of this scattering highly virtual photons will be radiated and can be interacting with photons which are emitted by the other beam particle. The increase of the photon emission probability with the increase

of the beam-particle's energy makes LEP a source of γ's with continuous energy. Its cross-section is much higher than in any previous e^-e^+-storage ring. Altogether, this fact allows to obtain photon fluxes of high intensity; however, the "beam-energies" of such photons can not be controlled.
The investigation of lepton pair production is a Quantum-Electrodynamics (QED) process (Fig. 1, left), of the order $\mathcal{O}(\alpha^4)$, where α is the Fine-Structure Constant. The study of

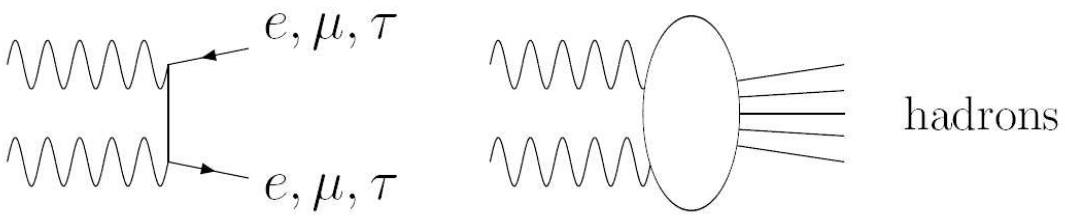

Figure 1: Inelastic processes for $\gamma\gamma$ scattering, left: QED, right: QCD.

$e^-e^+ \rightarrow e^-e^+\gamma\gamma \rightarrow e^-e^+l^-l^+ (l = e, \mu, \tau)$ allows to establish procedures to be adopted to studies in hadronic photon structure functions. However, although the production of final states with $e^\pm$, $\mu^\pm$, and $\tau^\pm$ have been measured, only the muonic case is feasible to extract the structure function from data [1].
The information of the kinematics of this process can be obtained by experimental observation, since the final state particles can be completely detected, in contrast to many QCD processes. Thus, the study of lepton pair production from $\gamma\gamma$-collisions will, besides supplying another test of QED, provide important tools for the application in QCD studies.

3 Two-photon scattering

The measurements of the structure functions of photons can be performed for three special cases due to experimental constraints [2]. The theoretical description as well as the measurements for these cases will be quite different. One distinguishes between

1. Single tagging
2. Anti-tagging
3. Double tagging

The differences for the cases are incumbent upon the measurement of the so called tagged electrons[1]. The measurements for the different cases define the *virtuality* of the radiated photons. The virtuality is a measure for the magnitude of the negative invariant masses squared of the photons and thus a measure how far the photon is off its mass-shell. This quantity is calculated from the squared four-momentum transfers of the electrons to the radiated photons, which are described by Q^2 respectively P^2, see Fig. 2. The configuration for the measure-

[1]Since the electron and positron behave identical in terms of two photon physics only the term *electron* will be used in the following.

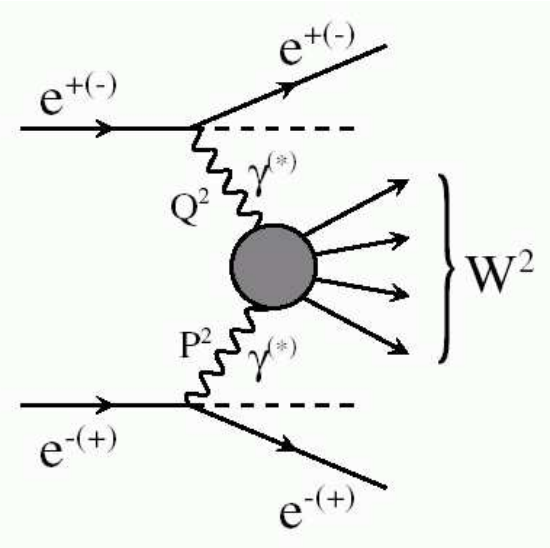

Figure 2: Two-photon production and scattering.

ment described herein is case 1: one of the scattered electrons is observed within an angular range $\theta_{low} < \theta_1 < \theta_{up}$, while the other electron is not observed over the angular range $\theta_{max} < \theta_2 < \pi - \theta_{max}$. This means, that the first electron is detected and precisely measured within a detector system with limited acceptance, whereas the second electron is considered being scattered into the cone with $\theta_2 < \theta_{max}$ or $\theta_2 > \pi - \theta_{max}$. If the angle θ_{max} is sufficiently small, the second electron will not be detected and is considered to be escaped close to the beam line, i.e. outside the detector acceptance. Hence, case 1 classifies a direct accessible $\gamma\gamma^*$ collision, since the four-momentum transfer to one photon will vanish, e.g. $P^2 \sim 0$ (quasi-real), whereas Q^2 is measured. The asterisk is used for virtual photons.
An additional feature of the QED treatment of $\gamma\gamma$-collisions is the access to further structure functions: $F_A^{\gamma,QED}$ and $F_B^{\gamma,QED}$, which correspond to transitions of photons with spin-flip (Fig. 3). The helicity is defined by the spin component in the direction of motion. Since real photons are massless, they cannot have a component parallel to their motion, i.e. they do not have a longitudinal, but only a transversal component. Virtual photons are off the mass-shell. This means, they can have a longitudinal polarization and therefore a non-zero helicity.
Since one photon is quasi-real, i.e. $m_\gamma \equiv 0$ in the case of single tagging, it does not have a longitudinal polarization. This photon is considered to be the target photon, whereas the other is the photon, which probes the structure of the target photon. Thus, the three amplitudes A_1, A_2, and A_3 are the only ones, which are independent from each other. In Fig. 3 one can schematically see the construction of the parameters A_i out of the total photon helicity states λ.
A_1 is described with the terms, (Fig. 3 from left to right) for $\lambda = 0, 2, 1$. A_2 and A_3 are made up by interference terms. These coefficients are related to $F_2^{\gamma,QED}$, $F_A^{\gamma,QED}$ and $F_B^{\gamma,QED}$ (see [3]).

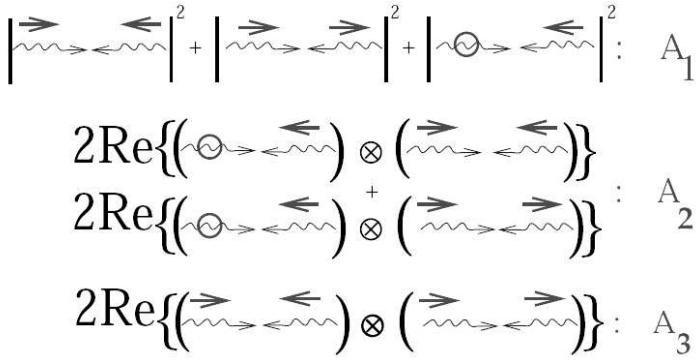

Figure 3: Helicity states for a single-tag configuration in two-photon collisions. The arrow depict the transverse helicity states, the circle the longitudinal helicity state of the probe photon.

4 Cross section and structure function

The differential cross-section can be then written in terms of cross-sections σ_{ab} and transition amplitudes τ_{ab} (see [4, 5]):

$$\begin{aligned} d\sigma &= K\Big(2|\rho_1^{+-}\rho_2^{+-}|\tau_{TT}\cos 2\tilde{\phi} \\ &\quad -8|\rho_1^{+0}\rho_2^{+0}|\tau_{TL}\cos\tilde{\phi} + 2\rho_1^{++}\rho_2^{00} \\ &\quad \times\big\{F_2(W,q_1^2,q_2^2)/D \\ &\quad -F_1(W,q_1^2,q_2^2)/C\big\} \\ &\quad +4\rho_1^{++}\rho_2^{++}F_1(W,q_1^2,q_2^2)/C\Big) \\ &\quad \times\frac{d^3p_1'd^3p_2'}{E_1E_2} \end{aligned} \tag{1}$$

where

$$\begin{aligned} F_1 &= \frac{\sqrt{\nu^2-q_1^2q_2^2}}{4\pi^2\alpha}(\sigma_{TT}-\frac{1}{2}\sigma_{TL}) \\ F_2 &= \frac{\nu|q_1^2|}{4\pi^2\alpha\sqrt{\nu^2-q_1^2q_2^2}} \\ &\quad \times\left(\sigma_{TT}+\sigma_{LT}-\frac{1}{2}(\sigma_{LL}+\sigma_{TL})\right) \\ &\quad \text{with } \nu = q_1\cdot q_2 \end{aligned} \tag{2}$$

The factors K and ρ_i depend on the four-momentum transfers, i.e. the measurable quantities p_i and q_i only, and the index T, L correspond to transversal and longitudinal polarization, respectively.
The structure-function F_2^γ can be accessed with a Monte-Carlo generator, which produces events according to (1). The basic idea of extracting F_2^γ is to set this parameter as a fixed value in the program and compare the measured differential cross-section with it. In other words,

one normalizes the structure-function to a fixed differential cross-section, say, $1\,nb$, and refers to the measured cross-section. The ratio of the differential cross-section and the normalized differential cross-section uncovers F_2^γ.
This can in principle be done with MC generators, like `VERMASEREN` [6], by means of modifying the program such, that it generates events according to $F_2 = 1\,nb$. However, there exists a Monte Carlo program, `GALUGA` [7], which can be used in a very convenient way.
It calculates the differential cross-section for $e^-e^+ \to e^-e^+X$ at given two-photon invariant mass W, or integrated over W. This cross-section is rewritten in terms of the photon virtualities q_i as the outermost integration variables (next to W), in order to simultaneously cope with anti-tagged and tagged electron modes.

5 Data analysis

The analyzed data sample was taken with the L3 detector at LEP/CERN in the years 1998-2000. The c.m.s. energy was between $189\,GeV$ and $208\,GeV$. The total integrated luminosity for the data sample used, was $\mathcal{L} = 600.2\,pb^{-1}$. The data sample was selected with single tag mode, i.e. only one electron had to be seen in the detector. Furthermore, the tagged electron had to be detected within the VSAT sub-detector ([8]) respectively the LUMInosity detector ([9]) of L3. The VSAT had a polar angular acceptance of $5mrad \leq \theta \leq 12mrad$, and accordingly for the other side of the vertex position. The range for the squared four-momentum transfer was $0.2\,GeV^2 \leq Q^2 \leq 0.85\,GeV^2$.
The LUMI had a polar angular acceptance of $32.6mrad \leq \theta \leq 63.6mrad$, and accordingly for the other side of the vertex position.

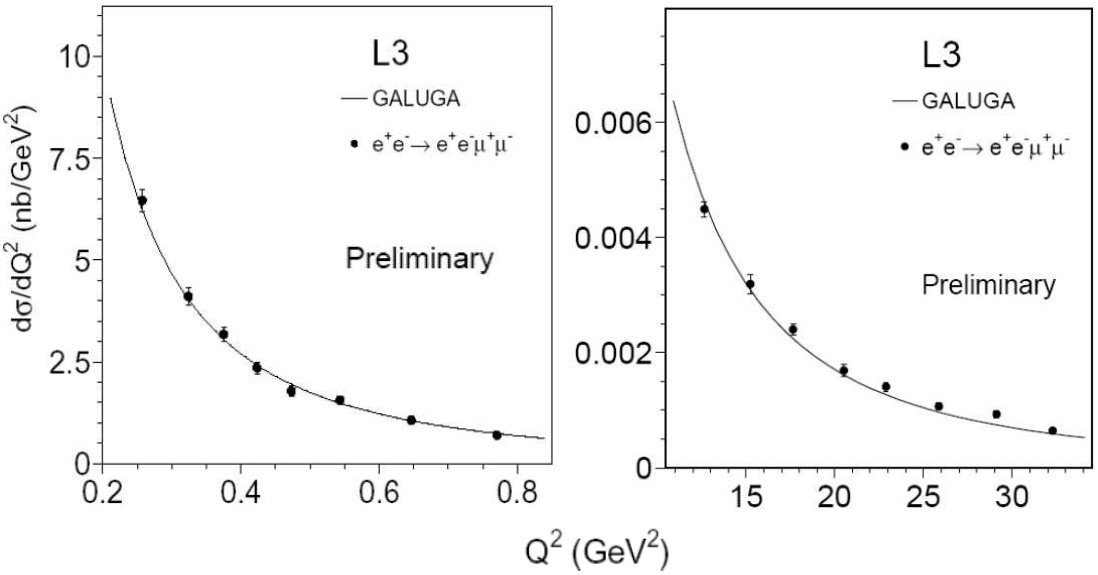

Figure 4: The differential cross-section as a function of Q^2 from the reaction $e^-e^+ \to e^-e^+\mu^-\mu^+$, left: with VSAT-tagged, right: with LUMI-tagged electrons. The QED curve has been obtained with the generator `GALUGA`. Only statistical errors are drawn.

The range for the squared four-momentum transfer was $11\,GeV^2 \leq Q^2 \leq 34\,GeV^2$.
The dimuon event was required to show exactly two well measured tracks where only one particle had to be identified as a muon in order to uniformly cover the angular range. The mean trigger efficiency for the years 1998 to 2000 was found to be $\varepsilon = 96.5 \pm 0.1\%$.

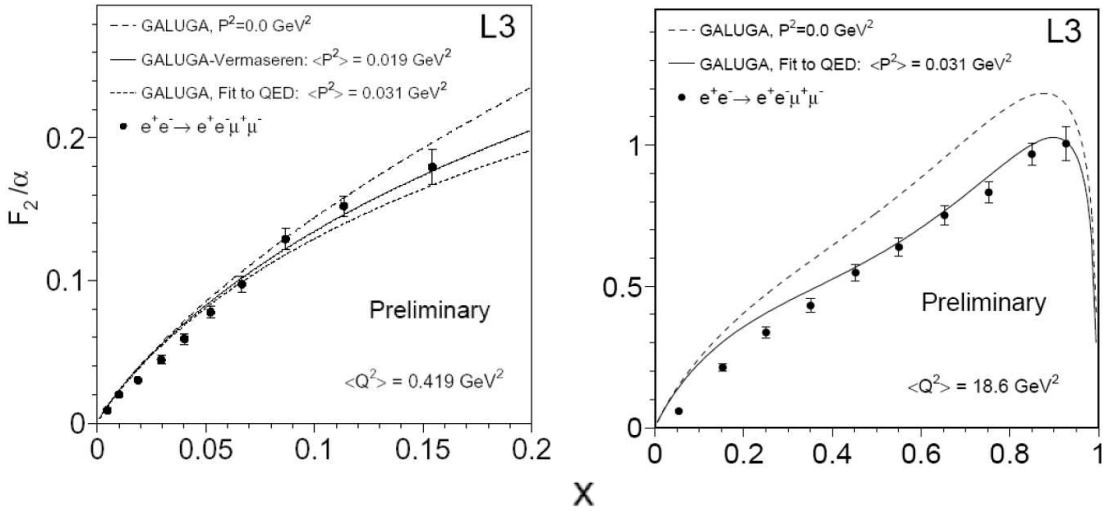

Figure 5: The structure function F_2 as a function of x from the reaction $e^-e^+ \to e^-e^+\mu^-\mu^+$, left: with VSAT-tagged, right: with LUMI-tagged electrons. The QED curves have been obtained with Eq.(2) and a mean virtuality of $P^2 = 0\,GeV^2$ (dashed line), $P^2 = 0.019\,GeV^2$ (solid line, MC), and $P^2 = 0.031\,GeV^2$ (dotted line, fit) for the target photon respectively. The data suggest that a non-zero virtuality should be used. Only statistical errors are drawn.

6 Results

The theoretical prediction of the differential cross-section was calculated with the MC generator `GALUGA`. Fig.4 shows a good agreement between data and the QED prediction. A series of differential cross-sections $d\sigma/dQ^2$ was calculated for a subdivision of Q^2-ranges within the range $0.2\,GeV^2 \leq Q^2 \leq 0.85\,GeV^2$ respectively for $11\,GeV^2 \leq Q^2 \leq 34\,GeV^2$. The crucial parameter used in `GALUGA` was the maximum polar angular range, in which the untagged electron can be scattered. The average Q^2 (center of gravity: c.o.g.) for each bin was calculated and the data points are depicted accordingly. The parameter x, which the structure function depends upon, is limited in its maximum to $x = 0.2$ for the VSAT-tagged sample. This is due to the fact that the range of Q^2 is rather small in connection with the minimum invariant mass of the two lepton event in its final state.
The measured structure function F_2 can be seen in Fig.5. There is a good agreement between data and prediction, based on Eq.(2). The structure function is suppressed as compared to non-vanishing virtualities of the probe photon. Although the effect of a non-zero virtuality of the target photon is not very significant at low x, the data suggest that $P^2 > 0\,GeV^2$. This becomes apparent for the case of higher four-momenta transfers (see Fig. 5 right). The average

value of $P^2 = 0.031 \pm 0.001\,GeV^2$ was obtained from a χ^2-fit procedure. A mean value of $P^2 = 0.019 \pm 0.001 GeV^2$ was obtained from the reconstructed MC sample for the VSAT-tagged sample.

References

[1] M. Krawczyk, M. Staszel, A. Zembrzuski. Phys. Rep. **345** (2001) 265.

[2] J.H. Field. "Lecture Notes in Physics: Photon Photon Collisions", v. **191** (1983) 270.

[3] G. Susinno Internal Report, L3 note 2193, 1997.

[4] V.M. Budnev, I.F. Ginzburg, G.V. Meledin and V.G. Serbo. Phys. Rep. **15**, (1975) 181.

[5] Ch. Berger and W. Wagner. Phys. Rep. **146**, (1987) 1.

[6] J.A.M. Vermaseren. Nucl. Phys. **B229** (1983) 347.

[7] G. A. Schuler Comp. Phys. Comm. **108** (1998) 279.

[8] F. Filthaut, F. Linde, T. van Rhee. Internal Report, L3 note 2117, 1997.

[9] I. C. Brock et al. Nucl. Inst. Meth. **A381** (1996) 236.